Cross comparisons of nuclear temperatures determined from excited state populations and isotope yields

M. B. Tsang, F. Zhu,* W. G. Lynch, A. Aranda,† D. R. Bowman,‡ R. T. de Souza,§
C. K. Gelbke, Y. D. Kim,‖ L. Phair,** S. Pratt, C. Williams, and H. M. Xu††
National Superconducting Cyclotron Laboratory and Department of Physics and Astronomy, Michigan State University, East Lansing, Michigan 48824

W. A. Friedman
Department of Physics, University of Wisconsin, Madison, Wisconsin 53706
(Received 23 October 1995)

Double ratios involving (^{6}Li, ^{7}Li, ^{3}He, ^{4}He) and (^{7}Li, ^{8}Li, ^{3}He, ^{4}He) isotope yields have been used to extract nuclear temperatures for the ^{36}Ar+^{197}Au systems at $E/A=35$ MeV. After correcting for sequential decays, these isotope temperatures are compared to corresponding temperatures obtained from excited state populations measured in the same experiment. Within experimental uncertainties, both techniques yield similar results.

PACS number(s): 25.70.Mn, 24.10.Pa, 25.70.Gh

Due to the short-range repulsion and mid-range attraction of nuclear forces, infinite nuclear matter displays a transition from a liquid to a gaseous phase [1–5], characterized by a mixed phase region at subnuclear densities and temperatures less than about 17 MeV. For finite nuclear systems, the manifestations of this phase transition are less obvious. Microcanonical calculations, however, surprisingly predict a peak in the heat capacity at excitation energies where such systems expand and undergo a multifragment decay via a ''cracking'' phase transition [6,7]. Experimental confirmation of such behavior merits a high priority.

Nuclear temperatures are generally determined from the distributions of emitted particles. Provided collective motion and preequilibrium emission may be neglected, the spectra of neutrons and light charge particles directly reflect the temperature of the systems from which they are emitted. For systems undergoing multifragment breakup, however, neither preequilibrium emission [8] nor collective expansion can be *a priori* neglected [9,10] and other techniques must be explored. Thermometers based upon the relative populations of excited states of emitted light nuclei have the advantage that they are insensitive to collective motion [11–16]. Such thermometers have been cross calibrated by measuring the decay of hot compound nuclei [17] and have been employed in investigations over a wide range of bombarding energies [11–16]. Systematic studies of excited state populations reveal only a gradual increase in temperature from 3 to 5.5 MeV as the incident energy is increased over the range from $30A$ to $200A$ MeV. This weak energy dependence is consistent with the assumption that the nuclear system cools by expansion [6,7,18] or particle emission [18]. While these observations are qualitatively consistent with the predictions of microcanonical calculations at moderate excitation energies, the sudden increase in the temperature at high excitation energies predicted by Microcanonical calculations for systems approaching the region of nuclear vaporization has not been observed so far [6,7].

Recently, nuclear temperatures have also been extracted from the relative yields of Li and He isotopes [19], assuming chemical and thermal equilibrium at freeze-out [20]. A series of measurements have been performed for ^{197}Au+^{197}Au collisions at an incident energy of $600A$ MeV as a function of the deduced excitation energy deposited in the projectile-like residue [19]. Similar to the temperatures extracted from excited state populations, a plateau of nearly constant $T=4.5$–5.5 MeV is observed for a wide range of deduced excitation energies, $2.5\ \text{MeV} \leqslant E^*/A \leqslant 10$ MeV [19]. At larger deduced excitation energies, $E^*/A > 10$ MeV, the temperature increases rapidly with excitation energy, following a relationship of $T \approx \frac{2}{3}(E^* - 2\ \text{MeV})$. This observation of a ''caloric'' curve characterized by a plateau followed by a rise in temperature qualitatively reproduces many of the essential predictions of microcanonical models [6,7]. It relies completely upon temperatures extracted from isotope ratios, however.

In the determination of the caloric curve in Ref. [19], temperatures were extracted from ratios of isotopic yields using the expression [19,20]:

$$T = \frac{B}{\ln(aR)}. \tag{1}$$

*Present address: Physics Department, Brookhaven National Laboratory, Upton, NY 11973.
†Present address: Physics Department, University of Texas, El Paso, TX 79968.
‡Present address: Chalk River National Laboratories, Chalk River, Ontario, Canada K0J 1J0.
§Present address: IUCF and Chemistry Department, Indiana University, Bloomington, IN 47405.
‖Present address: National Laboratory for High Energy Physics, 1-1 Oho, Tsukuba, Ibaraki 305, Japan.
**Present address: Lawrence Berkeley Laboratory, Berkeley, CA 94720.
††Present address: Cyclotron Institute, Texas A&M University, College Station, TX 77843.

Here, R denotes the measured ratio of isotopic yields, B is a binding energy parameter, and a depends on the nuclear spins. The latter two parameters were calculated by assuming that the relative yields of nucleus of charge Z_i and A_i are given by the corresponding ground state yields of these nuclei under the assumption of thermal equilibrium. In the approximate expression utilized by Refs. [19,20],

$$R=\frac{Y(A_i,Z_i)/Y(A_i+1,Z_i)}{Y(A_j,Z_j)/Y(A_j+1,Z_j)}, \tag{2}$$

$$B=BE(A_i,Z_i)-BE(A_i+1,Z_i)-BE(A_j,Z_j)+BE(A_j+1,Z_j), \tag{3}$$

$$a=\frac{[2S(A_j,Z_j)+1]/[2S(A_j+1,Z_j)+1]}{[2S(A_i,Z_i)+1]/[2S(A_i+1,Z_i)+1]}\left[\frac{A_j/(A_j+1)}{A_i/(A_i+1)}\right]^{\eta}, \tag{4}$$

where $Y(A_i, Z_i)$, $BE(A_i, Z_i)$, and $S(A_i, Z_i)$ are the measured total yield, the known binding energy and spin of the ground state of a specific isotope with mass A_i and charge Z_i. The exponent η arises from an integration over the energy spectrum and equals 1.5 in the limit of volume emission, and 1.0 in the limit of surface emission.

Temperatures extracted from the relative yields of isotopes can be strongly influenced by the fact that Coulomb and collective energies are mass dependent [9,10,21] while the thermal energy is not. The energy spectra of different isotopes may display different slopes. Such effects do not influence temperatures extracted from the relative populations of excited states. Since the sensitivities of the two techniques to the sequential decay of heavier particle unstable nuclei that feed the measured yields are different, a cross calibration of the two techniques is relevant. For this purpose we extract isotope temperatures for the ^{36}Ar+ ^{197}Au reaction at 35A MeV and compare them to temperatures extracted from excited states populations measured for the same experiment [22,23].

The experiment was performed at the National Superconducting Cyclotron Laboratory at Michigan State University. Beams of ^{36}Ar ions at 35A MeV from the NSCL K500 cyclotron bombarded ^{197}Au targets of 1 mg/cm^2 aerial density in the 92″ scattering chamber. Isotopes from $Z=1$ to $Z=5$ were measured with an array of 13 closely packed position sensitive gas-ΔE-E telescopes. Four of the telescopes located at $\theta_{\rm lab}=33.7°$ and 45.1° were optimized to detect charge particles with $Z>2$ (HF) and the remaining telescopes were optimized to measure light charge particles. As the present ratios involve lithium fragments, data detected with the HF telescopes will be primarily used. Each HF telescope subtended a solid angle of 5.6 msr and consisted of 75 μm and 100 μm thick surface-barrier silicon ΔE detectors and a 5 mm lithium-drifted Si(Li) E detector.

In addition to the hodoscope, the associated charge particle multiplicity was measured with the MSU Miniball [23,24] which covered 77% of 4π. Data from the combined array were analyzed in Refs. [22,23] to study the impact parameter dependence of temperatures extracted from the excited state populations. Futher details about the experimental set up and the algorithms used in defining central collision

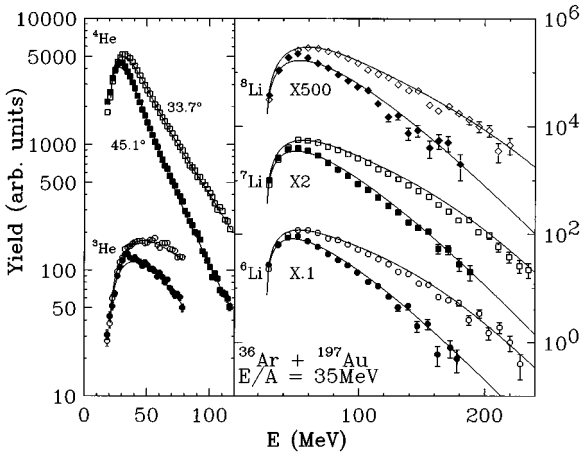

FIG. 1. Energy spectra for ^{3}He, ^{4}He (left-hand panel) and ^{6}Li, ^{7}Li, ^{8}Li (right-hand panel) at $\theta_{\rm lab}=33.7°$ and 45.1°. The solid lines are fits from three moving sources [23].

events are given in Ref. [23]. Examination of the excited states popuplation for this reaction revealed that the populations were more consistent with thermal equilibrium for central collisions with reduced impact parameter $\hat{b}=b/b_{\rm max}\leqslant 0.3$ than for peripheral collisions with $\hat{b}\geqslant 0.6$ [23]; $b_{\rm max}$ corresponds to the maximum impact parameter with an average charged particle multiplicity of 2. The data presented here were obtained for a reduced impact parameter $\hat{b}\leqslant 0.3$.

Figure 1 shows the energy spectra of ^{3}He, ^{4}He, ^{6}Li, ^{7}Li, ^{8}Li isotopes measured with the heavy ion telescopes at $\theta_{\rm lab}=34°$ and 45°. The ^{3}He spectra are truncated at 90 MeV due to the finite thickness of the 5 mm Si(Li) detectors. In general, the energy spectra at forward angles have higher cross sections and the slopes are less steep. The energy spectra of the three Li isotopes have similar shapes but the ^{3}He and ^{4}He energy spectra differ significantly. Such difference has been observed previously [25]. The steeper slopes of the alpha particles may arise from the enhanced secondary emission of ^{4}He relative to ^{3}He at later times and lower temperatures due to its larger binding energy. These differences in the spectral shapes can cause the measured isotope temperatures to depend strongly on the range of kinetic energies of the helium isotopes included in the isotope yields used in Eq. (1).

Temperatures were extracted using two different sets of isotopes: (^{6}Li, ^{7}Li, ^{3}He, ^{4}He) which was also used in Ref. [19] and a second set (^{7}Li, ^{8}Li, ^{3}He, ^{4}He). These two double isotope ratios are plotted in Fig. 2 for fragments of kinetic energy 0 MeV$\leqslant E\leqslant E_{\rm cut}$ MeV as a function of the cutoff energy per nucleon, $E_{\rm cut}/A$. The solid and open points are the ratios extracted directly from the measured yields. The values for R at $\theta_{\rm lab}=34°$ and 45° coincide; no significant angular dependence of the isotope ratios is observed within the experimental uncertainties and the limited angular coverage. To assess the effect of incomplete phase space coverage in the experiment, simulations were performed assuming a single moving source with 5 MeV temperature and source velocity of 0.1c. (The source velocity is chosen to be similar to those obtained in single source fits.) The kinematic effect of the experimental acceptance on the isotope yield ratio R is less than 10%.

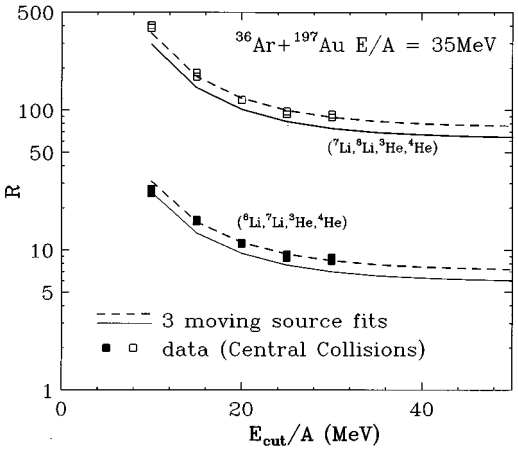

FIG. 2. The ratios of isotope yield as a function of the upper cut-off energy for two isotope groups. The experimental points include data from two angles, $\theta_{lab}=33.7°$ and 45.1° while the lines are extracted from energy spectra of the moving source fits at $\theta_{lab}=45°$.

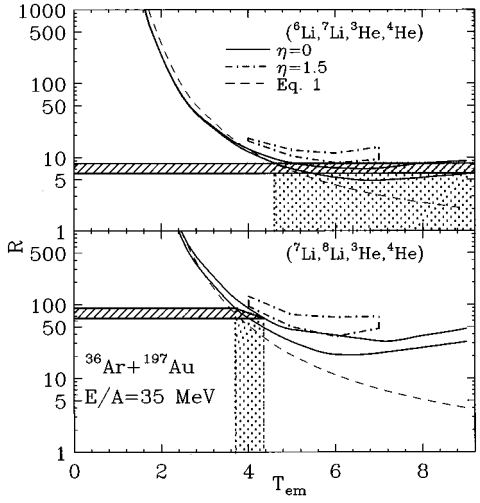

FIG. 3. The isotope yield ratios derived from sequential calculations is plotted against the input temperature, T_{em}. The horizontal hatched areas indicate the measured isotope yield ratios and the vertical shaded areas indicate the range of the extracted isotope temperatures. See text for the detailed description of the solid, dot-dashed, and dashed curves.

Since the yield of all particles drops off at higher energies, R attains asymptotic values as E_{cut}/A is increased. To extrapolate the energy spectra to higher energies, the energy spectra were fitted with nonrelativistic Maxwell distributions, assuming three moving sources as described in detail in Ref. [23] (solid lines in Fig. 1). These fits are used strictly to extrapolate the isotope yield ratios at high energies, they should not be interpreted literally as emission from moving sources, nor can they be used to accurately extrapolate to unmeasured scattering angles. (Single source fits are similar to the three source fits around the region of maximum yield and the R values obtained with single source fits are nearly the same as those obtained from the three source fits.) The extracted R values do not appear to be too sensitive to the uncertainties in the extrapolation of the helium spectra to higher energies.

The solid lines in Fig. 2 are determined by integrating the moving source fits for $\theta_{lab}=45°$ where the calculations and data closely agree. The discrepancies between data and the moving source fits mainly arise from inaccuracies in the fits at the low energies near the Coulomb barrier. For both isotope groups, the ratios are the lowest for the most energetic particles and increase with decreasing E_{cut}/A. This could reflect either an evaporative or a nonequilibrium cooling mechanism by which the most energetic particles are emitted at an early stage from the system when it is hottest. It would be very interesting to further explore this effect using telescopes of a greater dynamic range. Here we will focus upon average temperatures.

To extract the experimental asymptotic R values, the dashed lines are obtained by renormalizing the solid lines to the experimental data at $E_{cut}/A=30$ MeV. Taking into account uncertainties in the moving source fits, possible contamination of the ^{7}Li energy spectra by the alpha decay of ^{8}Be ($<4\%$) and the kinematic uncertainties arising from limited angular coverage in the measurement, a systematic uncertainty of 15% is assigned to the extracted values.

In the sequential calculations described in Refs. [22,23] particles are assumed to be emitted at freeze-out by a thermalized source of temperature T_{em}. In these calculations, the population of an excited state of a nucleus at excitation energy E_i^*, spin J_i, mass number A_i, and charge number Z_i was assumed to be of the form

$$P_i(A_i,Z_i,E_i^*,f,T_{em}) \propto (2J_i+1)A_i^{\eta}\exp\left(-f\frac{V_i}{T_{em}}+\frac{Q_i}{T_{em}}\right)\exp(-E_i^*/T_{em}), \quad (5)$$

where V_i is the Coulomb barrier and Q_i separation energy. All the tabulated low-lying discrete states as well as the unstable states in the continuum up to the maximum excitation energy of $4.6A$ MeV were included in the calculations. η was set to zero for the calculations published in Ref. [23]. Calculations were performed with trial initial temperatures, T_{em}, ranging from 1 to 9 MeV in 1 MeV steps [23]. At each value of T_{em}, the factor f was adjusted to make the final charge distributions agree with the experimentally measured ones [23]. This latter requirement provides an essential constraint on the actual amount of sequential feeding in the calculations [13,22,26]. At each temperature, unknown spins and parities of tabulated discrete states included in the calculation were also randomly assigned and calculations were repeated 10 times to assess the uncertainties in the calculations.

Sequential decay calculations for isotope double ratios for the groups (^{6}Li, ^{7}Li, ^{3}He, ^{4}He) and (^{7}Li, ^{8}Li, ^{3}He, ^{4}He) are given in the upper panel and lower panels of Fig. 3, respectively. Two solid curves shown in each panel bound the range of values of R obtained by varying the unknown spins and parities of discrete states [23] as a function of the emission temperatures, T_{em}. Beyond $T_{em}>4.5$ MeV, corrections due to sequential decay become extremely important and R flattens out and even increases slightly. This latter increase indicates potential problems with the extraction of temperatures higher than $T_{em}>4.5$ MeV from the isotope ratio method in this reaction. The importance of feedings at high

energies can be clearly demonstrated if one compares these calculations (solid curves) with calculations using Eqs. (1)–(4) without feeding corrections (dashed lines). Same sequential decay calculations indicate that the relative population of the widely separated ^{5}Li (g.s.) and ^{5}Li* (16.66 MeV) states allows the extraction of temperatures up to 6 MeV in this system [23]. Because the charge distributions for ^{36}Ar+^{197}Au collisions are relatively flat at $E/A=35$ MeV [23], the influence of sequential feeding may be larger in these calculations than it would be at higher excitation energies where the charge distributions may be steeper. Thus, one cannot infer, from these calculations alone, an inability to extract higher temperatures in another reaction from this isotope ratio method. Indeed, it is necessary to recalculate these curves for each new reaction so as to reproduce the relevant observed charge distributions.

The experimental measured R obtained in Fig. 2 are plotted as horizontal bars in Fig. 3. From the intersection of the data and the calculations, the relative isotope yields of (^{6}Li, ^{7}Li, ^{3}He, ^{4}He) provide an isotope temperature, $T_{\rm em}>4.6$ MeV while the isotope yields for (^{7}Li, ^{8}Li, ^{3}He, ^{4}He) give $T_{\rm em}=4.0\pm0.3$ MeV. In the present experiment, there is at least one other group of isotopes (d, t, ^{3}He, ^{4}He) that has a large enough binding energy difference, B, so as to permit the extraction of a useful isotope temperature. This isotope group was detected with the light ion telescopes and suffered from upper energy cutoffs at 40 and 45 MeV for deuterons and tritons, respectively. Nevertheless, an extrapolation with moving source fits was performed which yielded an isotope temperature of 4.2 ± 0.5 MeV, very similar to the one obtained for the (^{7}Li, ^{8}Li, ^{3}He, ^{4}He) group. Other isotope groups like (^{6}Li, ^{7}Li, ^{7}Li, ^{8}Li) have too small values of the binding energy difference, B, and are too sensitive to experimental and theoretical uncertainties to provide useful information.

We have also investigated the influence of the assumed charge to mass ratios of the thermalized emitting system on the isotope ratios. Decreasing the charge to mass ratios of the emitting system up to 20% changes the ratio R by less than 10%, well within the uncertainties of the present calculations. Similarly, we have investigated the exponential term of A^η in Eq. (5). The dot-dashed lines in Fig. 3 enclosed the upper and lower limits of the corresponding sequential decay calculations with $\eta=1.5$ (corresponding to the case of volume emission) for 4 MeV$\leqslant T_{\rm em}\leqslant$7 MeV. Inclusion of this factor increases the calculated isotope yield ratios R by about 40% allowing only lower limits $T_{\rm em}>4.1$ MeV and $T_{\rm em}>6$ MeV to be extracted for (^{7}Li, ^{8}Li, ^{3}He, ^{4}He) and (^{6}Li, ^{7}Li, ^{3}He, ^{4}He) isotope groups, respectively. For surface emission, $\eta=1$ (not plotted in Fig. 3), the increase in R is slightly less, about 30%, and the shift is correspondingly less. The sensitivity of the isotope temperatures to η represents an uncertainty that merits further study. The temperature obtained in Ref. [23] from the excited state populations of lithium, beryllium, and boron isotopes in the same reaction is 4.5 ± 0.5 MeV. This result is comparable to the temperatures extracted from the isotope ratios.

In summary, comparison of isotope temperature measurements with excited state temperature measurement for the reaction ^{36}Ar+^{197}Au at $E/A=35$ MeV indicates that the temperature obtained from the yield ratios of (^{7}Li, ^{8}Li, ^{3}He, ^{4}He) isotopes is consistent with that obtained from the excited state populations and seems to be less sensitive to the assumptions used in the sequential model calculations. The corresponding cross calibration of the measurement obtained with the (^{6}Li, ^{7}Li, ^{3}He, ^{4}He) isotopes is less satisfying because of the larger sensitivity to decay distributions. The current study suggests that more work is needed to cross check isotope temperatures at higher excitation energies and possibly with different isotope groups. A better understanding of the energy spectra and a determination of all the mass dependent factors in the fragment energy spectra would greatly improve the accuracy of the sequential decay calculations used in extracting these isotope temperatures.

This work was supported by the National Science Foundation under Grant Nos. PHY-89-13815 and PHY-92-14992.

[1] D. Q. Lamb *et al.*, Phys. Rev. Lett. **41**, 1623 (1978).
[2] H. Jaqaman, A. Z. Mekjian, and L. Zamick, Phys. Rev. C **27**, 2782 (1983); **29**, 2067 (1984).
[3] J. Kapusta, Phys. Rev. C **29**, 1735 (1984).
[4] A. L. Goodman, J. Kapusta, and A. Z. Mekjian, Phys. Rev. C **30**, 851 (1984).
[5] D. H. Boal and A. L. Goodman, Phys. Rev. C **33**, 1690 (1986).
[6] D. H. E. Gross, Phys. Rev. Lett. **56**, 1544 (1986).
[7] J. P. Bondorf *et al.*, Nucl. Phys. **A443**, 321 (1985); **A444**, 460 (1986).
[8] L. Phair *et al.*, Nucl. Phys. **A564**, 453 (1993).
[9] W. C. Hsi *et al.*, Phys. Rev. Lett. **73**, 3367 (1994).
[10] S. G. Jeong *et al.*, Phys. Rev. Lett. **72**, 3468 (1994).
[11] C. Schwarz *et al.*, Phys. Rev. C **48**, 676 (1993).
[12] J. Pochodzalla *et al.*, Phys. Rev. C **35**, 1695 (1987).
[13] T. K. Nayak *et al.*, Phys. Rev. C **45**, 132 (1992).
[14] G. J. Kunde *et al.*, Phys. Lett. B **272**, 202 (1991).
[15] C. B. Chitwood *et al.*, Phys. Lett. B **172**, 27 (1986).
[16] H. Xi *et al.*, Nucl. Phys. **A552**, 281 (1993).
[17] D. J. Morrissey, W. Benensen, and W. A. Friedman, Annu. Rev. Nucl. Part. Sci. **44**, 27 (1994), and references therein.
[18] W. A. Friedman, Phys. Rev. C **42**, 667 (1990).
[19] J. Pochodzalla *et al.*, Phys. Rev. Lett. **75**, 1040 (1995).
[20] S. Albergo *et al.*, Nuovo Cimento **89A**, 1 (1995).
[21] K. G. R. Doss *et al.*, Phys. Rev. Lett. **59**, 2720 (1987).
[22] F. Zhu *et al.*, Phys. Lett. B **282**, 299 (1992).
[23] F. Zhu *et al.*, Phys. Rev. C **52**, 784 (1992).
[24] R. T. DeSouza *et al.*, Nucl. Instrum. Methods Phys. Res. Sect. A **295**, 109 (1990).
[25] K. G. R. Doss *et al.*, Mod. Phys. Lett. A **3**, 849 (1988).
[26] H. M. Xu *et al.*, Phys. Lett. B **182**, 155 (1986).